THE ROYAL SOCIETY

Received 5 April 2004
Accepted 17 May 2004
Published online 24 September 2004

Mortality in cultures of the dinoflagellate *Amphidinium carterae* during culture senescence and darkness

Daniel J. Franklin* **and John A. Berges†**

School of Biology and Biochemistry, The Queen's University of Belfast, 97 Lisburn Road, Belfast BT9 7BL, Northern Ireland, UK

The study of cell death in higher plants and animals has revealed the existence of an active ('programmed') process in most types of cell, and similarities in cell death between plants, animals, yeast and bacteria suggest an evolutionarily ancient origin of programmed cell death (PCD). Despite their global importance in primary production, information on algal cell death is limited. Algal cell death could have similarities with metazoan cell death. One morphotype of metazoan PCD, apoptosis, can be induced by light deprivation in the unicellular chlorophyte *Dunaliella tertiolecta*. The situation in other algal taxa is less clear. We used a model dinoflagellate (*Amphidinium carterae*) to test whether mortality during darkness and culture senescence showed apoptotic characteristics. Using transmission electron microscopy, fluorescent biomarkers, chlorophyll fluorescence and particulate carbon analysis we analysed the process of cell mortality and found that light deprivation caused mass mortality. By contrast, fewer dead cells (5–20% of the population) were found in late-phase cultures, while a similar degenerate cell morphology (shrunken, chlorotic) was observed. On morphological grounds, our observations suggest that the apoptotic cell death described in *D. tertiolecta* does not occur in *A. carterae*. Greater similarity was found with paraptosis, a recently proposed alternative morphotype of PCD. A paraptotic conclusion is supported by inconclusive DNA fragmentation results. We emphasize the care that must be taken in transferring fundamental paradigms between phylogenetically diverse cell types and we argue for a greater consistency in the burden of proof needed to assign causality to cell death processes.

Keywords: apoptosis; lysis; morphology; mortality; necrosis; programmed cell death

1. INTRODUCTION

Phytoplankton cell lysis is important in aquatic biomass cycling (Walsh 1983; Brussaard *et al.* 1995; Agusti *et al.* 1998; Kirchman 1999) and often constitutes a significant source of organic carbon (e.g. Noji *et al.* 1986; Pollingher 1987; Van Boeckel *et al.* 1992; Heiskanen 1993; Brussaard *et al.* 1996). Despite its importance, cell lysis, and particularly the cellular processes involved in cell death, have been poorly studied in comparison with the causes of cell proliferation (Sheldrake 1974; Fogg & Thake 1987). By extension with metazoan cells, cell death could be 'active', i.e. resulting from protein synthesis and caspase (cysteinyl aspartate-specific proteinase) activation within moribund cells (Segovia *et al.* 2003). Active cell death is known as programmed cell death (PCD), and is thought to be a process found throughout all domains of living things (e.g. Ameisen 2002). The existence of PCD among unicellular eukaryotes is at first counterintuitive, because PCD lacks an obvious adaptive role in unicellular organisms, and may therefore be the result of viral–eukaryote genomic mixing during ancient evolutionary history (Berges & Falkowski 1998; Segovia *et al.* 2003). A converse of active cell death, passive cell death or necrosis, is similarly well described in metazoan cells. Necrosis is passive because it requires no new gene expression in the moribund cell.

PCD is mediated by the cell itself through the expression or activation of specific proteins within the moribund cell. Caspases are thought to be the principal enzyme family responsible for the morphological changes which are then manifest within the dying cell (Cohen 1997; c.f. Vaux & Korsmeyer 1999). Apoptotic morphotypes can result from PCD, and markers considered to indicate apoptosis include DNA fragmentation, chromatin condensation, cell shrinkage, formation of apoptotic bodies (containing intact organelles), membrane 'blebbing' and phosphatidylserine inversion. Necrotic cells, by contrast, show a loss of plasma membrane integrity, swelling and then lysis (Kerr *et al.* 1972; Wyllie *et al.* 1980). Protein synthesis is not necessary for necrosis to occur and, in comparison with apoptosis, necrosis can be quite rapid, e.g. seconds to minutes (Willingham 1999). Deviations from these two major paradigms have been found. In mouse fibroblast cells, cell death can be triggered by a molecular signal resulting in extensive vacuolization and mitochondrial swelling; this process, called paraptosis, is distinct from apoptosis because it occurs without nuclear fragmentation, apoptotic body formation and chromatin condensation (Sperandio *et al.* 2000). The widening of cell death study to encompass

*Author and address for correspondence: School of Environmental Sciences, University of East Anglia, Norwich NR4 7TJ, UK (dan.franklin@uea.ac.uk).
†Present address: Department of Biological Sciences, University of Wisconsin–Milwaukee, 3209 North Maryland Avenue, Milwaukee, WI 53211, USA.

phylogenetically diverse cell types has highlighted the necessity of multiple biomarkers in the assessment of cell death. For example, limitations in the assays used to assign an active cell death process, e.g. DNA fragmentation (see Graslkraupp *et al.* 1995; Kanduc *et al.* 2002), demonstrate the importance of collecting a wide spectrum of data to aid in interspecies comparisons.

The unicellular chlorophyte *Dunaliella tertiolecta* undergoes mass cell death and lysis when placed in darkness (Berges & Falkowski 1998; Segovia *et al.* 2003). Importantly, *D. tertiolecta* mass cell death occurs in the absence of viruses, and is inhibited by broad-spectrum caspase inhibitors (Segovia *et al.* 2003). *Dunaliella tertiolecta* cells killed by darkness show a morphology consistent with metazoan apoptosis (Segovia *et al.* 2003): DNA fragmentation (as detected by the terminal deoxyribonucleotidyl transferase (TDT)-mediated dUTP-biotin nick end labelling (TUNEL) assay (Gavrieli *et al.* 1992)), caspase activation, a distinctive nuclear morphology, and increased proteolytic activity (i.e. leucine aminopeptidase activity (LAP; e.g. Berges & Falkowski 1996)) are induced (Berges & Falkowski 1998; Segovia *et al.* 2003). Thus, *D. tertiolecta* cell death is probably the result of PCD (Segovia *et al.* 2003). To date, PCD has also been documented in two dinoflagellates (Vardi *et al.* 1999; Dunn *et al.* 2002) and a cyanophyte (Ning *et al.* 2002). While the findings that elements of a PCD process operate within chlorophytes, dinoflagellates and cyanophytes represent good progress, it should be remembered that all phytoplankton studies to date have used different stresses to kill cells, as well as different burdens of proof in the assessment of PCD.

Our objective was to characterize changes in the morphology, protease activity, variable fluorescence and DNA fragmentation of dying *Amphidinium carterae* cells to test the hypothesis that environmental stress (in the form of darkness and late-phase culture) could induce PCD in a dinoflagellate cell. We found similarities (vacuolization, lysis, loss of organelles) between dead *A. carterae* and *D. tertiolecta* cells, but the lack of DNA fragmentation, apoptotic body formation and chromatin condensation argue against *A. carterae* cell death being apoptotic. It is probably an 'active' process, as almost all cell death is (Jones 2001), but does not fit neatly into the paradigms developed to conceptualise metazoan cell death.

2. MATERIAL AND METHODS

(a) *Batch culture growth of* Amphidinium carterae *and dark treatment*

Amphidinium carterae (Hulbert 1957) was obtained from the Culture Collection of Algae and Protozoa (CCAP no. 1102/1; Dunstaffnage Marine Laboratory, Oban, UK) and grown in natural seawater L1 medium (Guillard & Hargraves 1993) in duplicate 1.5 l semi-continuous batch cultures. L1 medium was supplemented with boric acid, Tris buffer and sodium bicarbonate, following a modification of the Harrison recipe (see Berges *et al.* 2001). Cultures were grown at 16 °C under 200 μmol quanta $m^{-2} s^{-1}$, with an 18 L : 6 D cycle, until mid- to late-log phase. Cell numbers were estimated either with Lugols-fixed cell counts (duplicate Sedgewick-Rafter chambers) or, with live cells, using a Coulter counter (100 μm aperture tube, Model Z2, Beckman-Coulter, Fullerton, CA, USA). The size of cells was also recorded and collated into size classes. At mid- to late-log phase, cells were placed in darkness by wrapping cultures in multiple layers of foil and black cloth. For stationary phase observations, cultures were simply kept in the light. To test the viability of cells in darkness, subcultures were launched from dark cultures after 3 and 8 days and returned to the light. Regrowth was then followed by measuring fluorescence (see below).

(b) *Quantifying cell death using Sytox-green*

Sytox-green (Sytox, Molecular Probes, Leiden, Holland, cat. no. S-7020) is a mortal stain which tests the integrity of the plasma membrane: Sytox only passes across the plasma membranes of dead cells where it labels the nucleus a brilliant green (Veldhuis *et al.* 1997, 2001). Sytox-green staining may therefore indicate an early stage in cell death; clearly if lysis occurs and cells are lost, Sytox has nothing to label. Incubation time and stain concentration were optimized prior to use and assays were validated using heat-killed cells (typically killed by heating at 65 °C for *ca.* 1 h) to check that stain uptake was proportional to the quantity of dead cells (data not shown). Sytox working stocks were made by dilution with double-distilled water and stored at −20 °C. After addition of Sytox to a final concentration of 5 μM, 1 ml samples of culture were incubated in the dark at 20 °C, for 30 min. Sample fluorescence (stain uptake) was then either read in a spectrofluorometer (LS5, Perkin-Elmer, Norwalk, CT, USA) at an excitation of 488 nm and at 523 nm emission (slit widths of 10 nm) or viewed directly with an epifluorescence microscope (excitation 450–490 nm bandpass; emission 515 nm, longpass). For microscope counts, it was sometimes necessary to concentrate cells with centrifugation (4500 × *g*, at 16 °C for 5 min). Controls indicated that centrifugation did not kill the cells (data not shown). To estimate the proportion of dead cells in the culture two counts were made. First, the average number of dead cells per microscope field of view (FOV) was counted in a haemocytometer: between 100 and 400 dead cells (i.e. Sytox-stained cells) were counted. Because some live cells were motile, cells had to be fixed before counting the total number of cells. Samples were fixed with Lugols and total cells were counted, again yielding an average, this time the average number of fixed cells (i.e. total cells) per FOV. The percentage of dead cells was then calculated as: (mean number of dead cells FOV^{-1})/(mean number of fixed cells FOV^{-1}) × 100.

(c) *Photosynthetic capacity (dark-adapted $F_V : F_M$)*

Measurement of the quantum yield of fluorescence from photosystem II (PSII) (Samuelsson & Oquist 1977) allows rapid and sensitive characterization of cellular photosynthetic capacity. In laboratory cultures, the addition of 3-(3,4-dichlorophenyl)-1,1-dimethylurea (DCMU) inhibits photosynthetic electron transport and permits the measurement of maximal fluorescence (Cullen & Renger 1979). Eight millilitre culture samples were withdrawn daily and dark-adapted for 30 min to allow for dissipation of non-photochemical quenching. After dark adaption, F_O was measured with a bench-top fluorometer (TD-700 fluorometer, Turner designs, Sunnyvale, CA, USA): 50 μl of 10 mM DCMU was added, and F_M measured immediately. Photosynthetic capacity ($F_V : F_M$) was then calculated as $(F_M - F_O)/F_M$ (Cullen & Renger 1979).

(d) *Protease leucine aminopeptidase activity*

Duplicate 40 ml samples were harvested from each culture and centrifuged (4500 × *g*, at 4 °C for 5 min); the resulting pellets were recombined into a suspension within a 1.5 ml microcentrifuge tube using a Pasteur pipette and recentrifuged (3000 × *g*, at 4 °C

for 5 min), the supernatant was discarded and the pellet snap-frozen in liquid N_2 prior to storage at −70 °C. Depending on pellet size, between 100 and 250 µl of 50 mM Tris buffer (pH 7.5) was added to the pellets which were sonicated (25 W, Vibra-cell sonicator, Sonics and Materials Inc, Danbury, CT) with 6 × 10 s cycles on ice. The pellets were then refrozen in liquid N_2, briefly defrosted, and resonicated. Of the resulting homogenate, 2–5 µl was used for protein quantification using the bicinchoninic acid method (BCA-1 kit, Sigma Chemical Co., St Louis, MO (Smith *et al.* 1985)) and 25 µl was used for the LAP assay. Synthetic LAP substrate (2 mM L-leucine 7-amido-4 methyl coumarin in water; Sigma L-2145) was made up fresh, and 0.5 ml was added to 25 µl of the sample homogenate in 475 µl of 50 mM Tris buffer (pH 7.5). The resulting reaction was followed over 180 s in the time-drive mode of a spectrofluorometer (Perkin-Elmer LS5) set at 380 nm excitation, 460 nm emission with 10 nm slit widths. Calibration standards (10 and 100 nM) were run with 7-amido-4 methyl coumarin (the free-fluorescent cleavage product). Slopes were calculated over the linear range of the enzyme reaction and enzyme activity was then calculated in µmol of product min^{-1} mg $protein^{-1}$ (e.g. Berges & Falkowski 1996).

(e) *Elemental analysis for the determination of culture particulate carbon*

To test whether cell lysis was induced by darkness we measured the particulate carbon (PC) content of the cultures. Samples (10 and 5 ml) of culture were filtered onto pre-ashed (24 h at 450 °C), 13 mm glass fibre filters (Gelman type A/E, mean pore size 1 µm). Filter discs were then dried for 24 h at 45 °C, before being wrapped in tin-foil discs and stored until all samples had been collected. The samples were measured in an elemental analyser (Model NA1500, Carlo Erba Instruments, Italy), using acetanilide standards and correcting samples using filter blanks.

(f) *Bacterial and viral staining*

Because algal cell lysis can be induced by viral attack (Suttle *et al.* 1990) it was necessary to check the cultures for the presence of viruses. The stain SYBR-green (Molecular Probes, Leiden, Holland, cat. no. S-70203) allows detection of both viral and bacterial particles with epifluorescence microscopy (Noble & Fuhrman 1998). Duplicate 5 ml samples were analysed from the dark cultures three times in the week following darkness. The culture samples were fixed with 1% glutaraldehyde and stored at 4 °C until analysed (a maximum of two to three months). SYBR-green was made up fresh and added to samples according to Noble & Fuhrman (1998). Cells were filtered onto 0.2 µm Anodisc filters (Whatman, Maidstone, UK), backed by 0.8 µm type HA filters (Millipore Corp., Bedford, MA, USA), under gentle vaccuum (less than 5 mm Hg). Bacterial cells and viral particles were counted under epifluorescence microscopy with an oil immersion objective (magnification × 1250, excitation 450–490 nm bandpass, emission 515 nm longpass) using the antifade mountant of Noble & Fuhrman (1998).

(g) **Amphidinium carterae** *cell structure and ultrastructure (light and transmission electron microscopy*

Cells were collected as for protease activities (see above), and were then fixed for 2 h in 100 mM Na-cacodylate buffer containing 4% glutaraldehyde and 8.6% sucrose. Samples were taken from duplicate cultures before dark (mid-log phase cultures), 3 days after dark, and 8 days after dark. Samples were not taken from senescent cultures. The cell pellets were washed in 100 mM Na-cacodylate buffer of descending sucrose concentration (0.2, 0.1, 0.05 and 0 M) and post-fixed in 1% OsO_4 for 2 h. Following fixation, the cells were dehydrated in an ascending series of ethanol (70 to 100%) and embedded in epoxy resin (Agar scientific, Stansted, UK). The resin-embedded pellet was then polymerized for 48 h at 60 °C and sections of 60–100 nm were cut with an ultramicrotome (Ultracut E, Reichert, Bensheim, Germany) equipped with a diamond knife. Grids were stained with uranyl acetate and lead citrate, and observed under transmission electron microscopy (TEM) (100 CX, Jeol, Tokyo, Japan). A Leitz Dialux 20 microscope was used to make light and epifluorescence observations. During both the dark period and stationary phase, qualitative observations were made every day.

(h) *TUNEL labelling for the assessment of DNA fragmentation*

An *in situ* cell death detection kit (Roche diagnostics, Mannheim, Germany, cat no. 164795) was applied to *A. carterae* cells from dark, stationary and mid-log phase cultures. The cells were collected by centrifugation (4500 × *g*, 10 min; typically 20–40 ml of culture), and fixed in 1 ml of 4% paraformaldehyde in phosphate buffered saline (PBS) at 4 °C for 1.5 h. The cells were then washed in PBS before permeabilization (0.1% Triton X-100 in PBS) for 10 min on ice. Labelling followed kit instructions. TUNEL protocols typically recommend a positive control, made by cleaving DNA with DNase. We added DNase (DNase I, Sigma, cat no. D-4527) to the cells after permeabilization (according to the kit instructions), and incubated them at room temperature for 30 min. For unknown reasons, DNase-treated positive controls failed to stain despite numerous trials varying both DNase (1 and 10 µg ml^{-1} in the reaction buffer) and Triton X-100 (0.1 and 1%). The fixation period was also extended to an overnight period to test the idea that cross-linking activity was insufficient in a 1.5 h fixation period. Positive controls still did not label with the free nucleotides. As an alternative, to verify the protocol, we used *D. tertiolecta* cells collected from light-deprived cultures undergoing mass mortality; these have previously been shown to label well using the TUNEL protocol (see Segovia *et al.* 2003), and did so in the present study. For negative controls, double-distilled water was substituted for the terminal deoxynucleotidyl transferase enzyme (see Gavrieli *et al.* 1992) during the labelling steps. After labelling, the cells were filtered onto black polycarbonate filters (0.8 µm, Osmonics, Livermore, CA, USA). The filter was mounted on a glass slide with antifade mountant (Noble & Fuhrman 1998) and viewed under epifluorescence microscopy (excitation bandpass 450–490 nm, emission longpass 515 nm) using magnification × 1250 with an oil-immersion objective.

(i) *Esterase activity (fluorescein diacetate hydrolysis)*

Fluorescein diacetate (FDA) (Molecular Probes, Leiden, Holland, cat. no. F-1303) is a vital stain which diffuses into cells where it is cleaved (hydrolysed) by non-specific esterases to yield the fluorescent product fluorescein. Accumulations of fluorescein are therefore the result of intracellular esterase activity, and are taken to indicate viability (e.g. Jochem 1999). One millilitre samples of culture were withdrawn before and after darkness, and FDA added to a final concentration of 30 µM. Samples were incubated in the dark at 20 °C for 1 h, and then measured in a spectrofluorometer (LS5, Perkin-Elmer, Norwalk, CT, USA) set at 451 nm excitation and 510 nm emission, with excitation and emission slit widths set at 10 and 3 nm, respectively. Stain concentration and incubation times were optimized prior to use (data not shown).

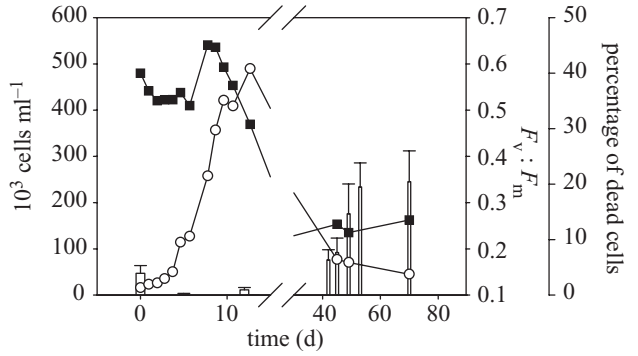

Figure 1. The growth (cell number (circles)), photosynthetic capacity ($F_V : F_M$ (squares) see text), and number of dead cells (bars) in *Amphidinium carterae* batch cultures grown at 16 °C under 200 μmol m^{-2} s^{-1}. The cell number and photosynthetic capacity data are drawn from a single representative culture, whereas the data for the number of dead cells was performed in a separate experiment and the bars represent the mean of duplicate cultures (±1 s.e.m.).

3. RESULTS

(a) *Growth, photosynthetic capacity and cell death of* Amphidinium carterae *in batch culture*

Amphidinium carterae cultures reached the stationary phase at *ca.* 4–5 × 10^5 cells ml^{-1}, with a specific growth rate (Fogg & Thake 1987) of *ca.* 0.4 μ d^{-1} during the log phase (figure 1). Cultures typically reached the stationary phase after *ca.* 15–20 days. On this basis, a population number of *ca.* 250 × 10^3 cells ml^{-1} was judged as representative of the mid-log phase point, and it was at this point that cultures were placed in darkness in subsequent experiments. Photosynthetic capacity ($F_V : F_M$) was stable between 0.5 and 0.6 during the log-phase, indicating that the cells were nutrient replete and photosynthetic performance (*sensu* Maxwell & Johnson 2000) was healthy. During the stationary phase (i.e. when cells had ceased to divide), $F_V : F_M$ declined to between 0.2 and 0.3 (figure 1). The measurement of F_O (dark-adapted chlorophyll fluorescence) closely followed cell number during exponential growth but continued to increase in exponential phase when the cell number was constant or declining (data not shown). Increases in cell fluorescence during the stationary phase meant that fluorescence was only reliable as a proxy for biomass during the log phase. During the stationary (senescence) phase, between 10 and 25% of cells stained as dead, over a period of 25 days (figure 1). The culture contained very few (less than 2%) dead cells during the period of rapid cell division (figure 1).

(b) *Effect of darkness on cell number, photosynthetic capacity, particulate carbon, bacterial biomass, cell death and culture protease leucine aminopeptidase levels*

Darkness halted cell division (figure 2*a*): when duplicate mid-log phase cultures were placed in darkness at a cell density of 2.5 × 10^5 cells ml^{-1}, the numbers of cells declined significantly (linear regression; $p < 0.05$) over the next 6 days to *ca.* 1.9 × 10^5 cells ml^{-1}. Upon being placed in darkness the photosynthetic capacity of these cultures decreased from a $F_V : F_M$ value of 0.6 to 0 within 3 days (figure 2*a*), indicating complete inactivation of the PSII reaction centre. The PC of duplicate cultures increased in tandem with cell division up to the transition to darkness; thereafter PC declined by 35% (from 22 to 14 mg ml^{-1}) in the 6 days following darkness (figure 2*a*). This decline in PC was significant (linear regression; $p < 0.05$), and

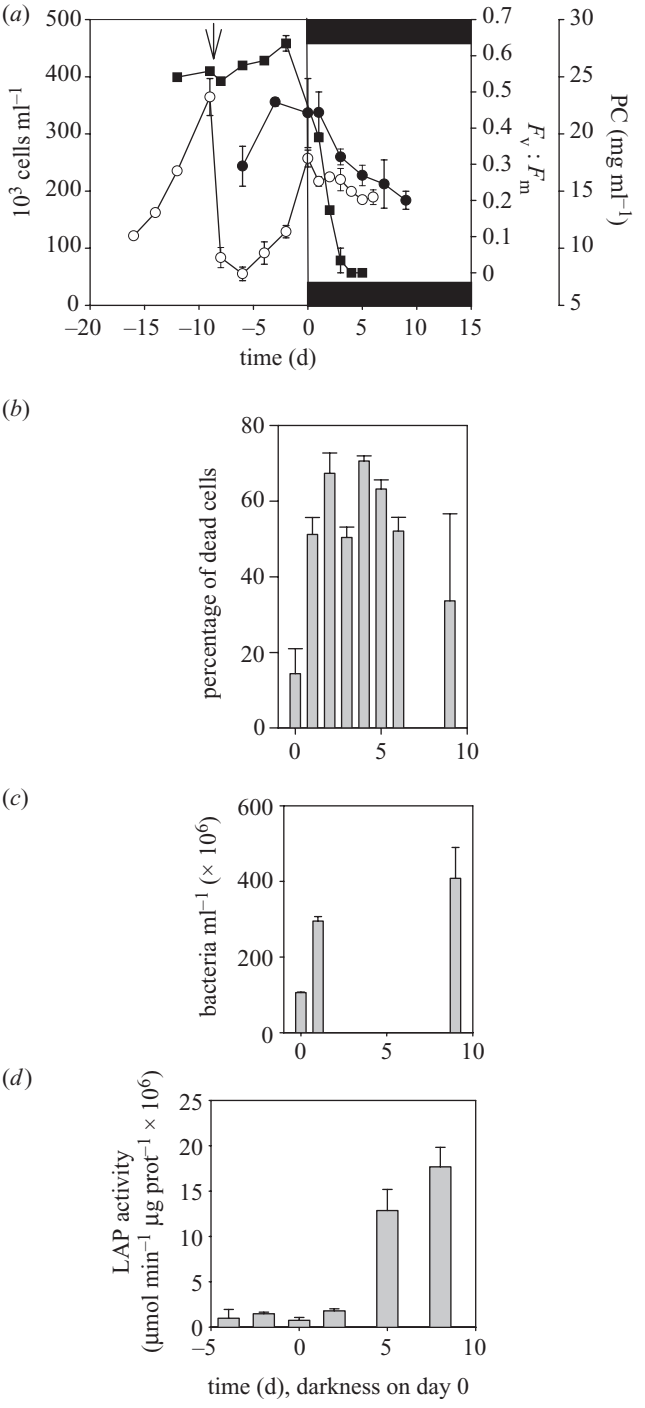

Figure 2. Effect of darkness on: (*a*) cell number (open circles), photosynthetic capacity ($F_V : F_M$ (squares)), and PC (closed circles); (*b*) number of dead cells (number of cells Sytox-stained; see text); (*c*) bacteria ml^{-1} (see text); and (*d*) culture protease (LAP; see text) levels, in duplicate *Amphidinium carterae* batch cultures. The black bars and vertical line in (*a*) represent the period of total darkness, and the arrow indicates when the cultures were diluted (on day −10). All data points represent the mean of duplicate cultures (±1 s.e.m.). The declines in cell numbers and PC after darkness were significant (linear regression; $p < 0.05$).

indicates that cell lysis occurred as a result of dark-induced mortality. The carbon : nitrogen ratio of these cultures declined from 5.6 to 4.1 over the 6 days in darkness, though this decline was not significant (linear regression; $p > 0.05$). The number of dead cells rose rapidly after darkness (figure 2*b*). A maximum of 75% of the cells were found to be dead—according to the Sytox staining technique—after 5 days in darkness. Duplicate sub-cultures from 3 day dark cultures resulted in regrowth of vegetative cells, after a short lag period. By contrast, duplicate sub-cultures from 8 day dark cultures produced no detectable growth (increases in fluorescence) over a three week monitoring period. The potential of dark cultures to regrow was tested twice with the same results. Over 9 days of darkness the number of bacteria in the cultures increased fourfold from 100×10^6 to 400×10^6 bacteria cells ml^{-1} (figure 2*c*), and the increased bacterial numbers (presumably supported by dinoflagellate lysis) was also noted in TEM and light observations. All bacterial cells were rod-shaped bacilli. Viruses were not observed. Cell protease levels (LAP) increased fivefold to sixfold in darkness (figure 2*d*), with the protease activity increase not apparent until 5 days after darkness.

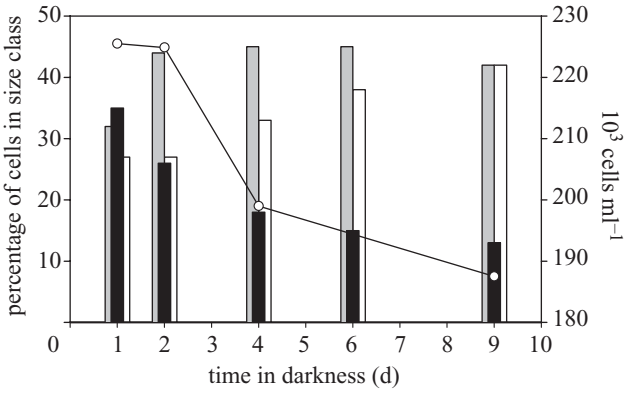

Figure 3. Effect of darkness on the size (bars) and number (points) of *Amphidinium carterae* cells in one log phase culture transferred to darkness on day 0. The bars represent the percentage of cells in the size classes 5–7 μm (open bars), 7–9 μm (grey bars), and 9–11 μm (black bars), as determined by Coulter analysis. A duplicate culture showed the same pattern: for clarity, the results from only one culture are displayed.

(c) *Effect of darkness on* Amphidinium carterae *cell morphology (light microscopy and transmission electron microscopy) and cell size*

A rapid change in cell morphology was induced by light deprivation. Throughout the log-phase, almost all cells appeared as the vegetative type: cells were motile and were dense with pigment. Dividing cells were seen very occasionally. When placed in darkness, cells became immotile and shrank: the number of cells in the 9–11 μm size class decreased from 35 to 12%, whereas the number of cells in the 5–7 μm class increased from 28 to 42% in the 9 days following the transfer to darkness. This cell shrinkage coincided with a decrease in the total number of cells (from 2.25×10^5 to 1.9×10^5 cells ml^{-1}; figure 3). Because cell shrinkage occurred simultaneously with cell loss and shrunken cells were absent before the stressful conditions, these data demonstrate that previously normal cells underwent cell shrinkage and that cell shrinkage led to cell lysis, as confirmed by the declines in PC.

TEM observations revealed cellular dissolution characterized by organelle loss. Pre-dark cells showed a full organelle complement with pyrenoids, starch, condensed chromosomes, nuclear and cell membranes all visible as well-defined structures (figure 4*a*,*b*), in agreement with previous ultrastructural studies (e.g. Dodge 1973). After 3 days of light deprivation many cells had deteriorated: vacuolization was apparent in some cells with intracellular contents becoming amorphous and lacking recognizable structure, although cell membranes appeared intact and smooth (figure 4*c*). At this point, 3 days after darkness, cells not substantially different from pre-dark cells were still seen (though this was not quantified by TEM). By day 8 of darkness only cell outlines were left in the vast majority of the cells examined (figure 4*d*) and a rise in bacterial numbers was apparent (sectioned bacterial cells were visible between dinoflagellate remains). Cells after 8 days in darkness were extensively vacuolated with only amorphous intracellular material remaining (figure 4*d*). A loss of pigment, leading to a chlorotic appearance, was obvious under both light and epifluorescent light (figure 4*f*, c.f. figure 4*h*) during the period of dark-induced mortality, and this was accompanied by the appearance of vacuolar spaces within chlorotic cells (figure 4*g*). However, vegetative cells were still seen at a very low frequency even after 6 days of darkness. In senescent cultures chlorotic cells (figure 4*f*) also appeared, and these cells stained with Sytox. Under light and epifluorescence microscopy, the morphology of dead cells produced in darkness and during senescence appeared similar (figure 4*f*, c.f. figure 4*g*), with simply the number of dead cells varying between the two treatments.

(d) *DNA fragmentation (TUNEL assay) during darkness and senescence*

DNA labelling, indicating the formation of strand breaks within nuclear DNA, was found in *D. tertiolecta* cells from light-deprived cultures. No labelling was found in *A. carterae* cells from senescent, light-deprived or mid-log phase cultures. In senescent and light-deprived cultures the morphological difference between dead chlorotic and live normal cells was clear under epifluorescence and light microscopy, although no differences in DNA labelling were apparent. *Amphidinium carterae* positive controls did not label with free nucleotides despite extensive trials varying the fixation period, DNase and Triton X-100 concentrations, and the strength of the reaction buffer. An alternative TUNEL assay (Apoptag fluorescein direct *in situ* apoptosis detection kit, Intergen, cat no. S7160), which works on the same principle (but using different proprietary components), was similarly trialled and also failed to label *A. carterae* cells after positive control treatment.

(e) *Esterase activity during darkness*

Relative esterase activity (i.e. fluorescein fluorescence) was proportional to cell number during cell growth. After darkness, the cultures showed an increase in esterase activity up to 10 days after the transition to darkness, whereupon esterase activity decreased to levels comparable with a control culture that had remained in the light (figure 5).

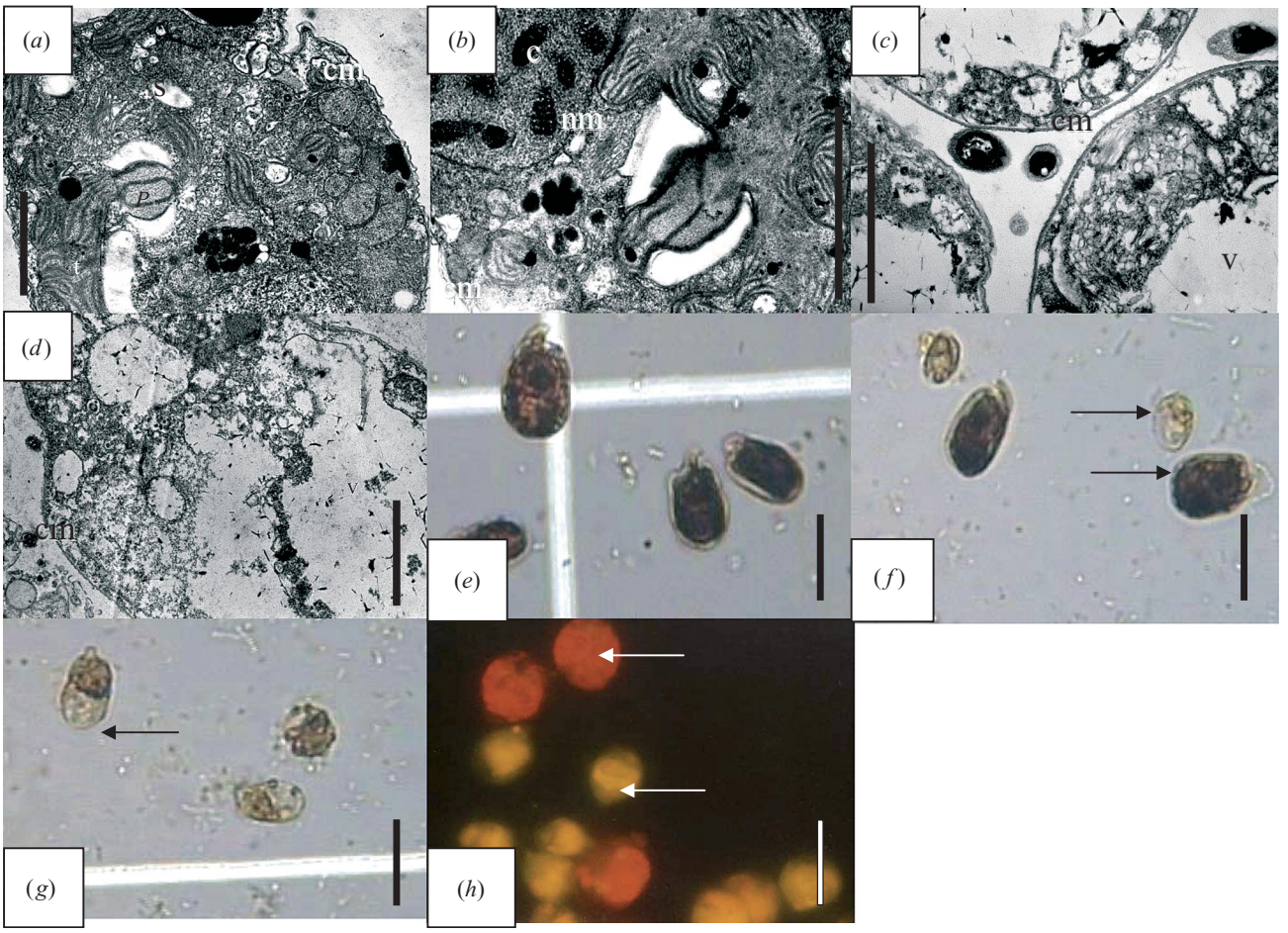

Figure 4. TEM and light microscope images of the effects of darkness on *Amphidinium carterae* morphology. (*a*) A single *A. carterae* cell from an exponential-phase culture in the light showing typical vegetative cell morphology including a starch-cap encased pyrenoid (P), thylakoid membranes (t), and starch grains (S). The cell membrane (cm) is also visible in this image, outlining the cell. (*b*) A slightly higher magnification image within a healthy cell, the nuclear membrane (nm) encloses regions of darkly-stained condensed chromosomes (c). Again, the cell membrane (cm) is visible. (*c*) Three degenerating cells lying alongside one another after 3 days in darkness: vacuoles (v) have appeared within the cells, although some cell material is still present around the margins of the cell. (*d*) After 8 days in darkness, the vast majority of cells contain only amorphous material and vacuoles (v) permeate the cell; here a single cell shows a complete loss of intracellular structure. In all TEM images the scale bar represents 1 μm. Under the light microscope, healthy cells (*e*) are pigment dense and show the typical vegetative cell outline with prominent epicones. In senescent cultures (*f*), vegetative cells persist alongside shrunken, chlorotic cells (see arrows), whereas in light deprived cultures (*g*), the vast majority of cells have died and have degenerated to the chlorotic state. The chlorotic state is obvious under epifluorescence microscopy (*h*), with a marked loss of red chlorophyll autofluorescence apparent in shrunken cells alongside normal, vegetative cells (see arrows). In all light or epifluorescence images the scale bar represents *ca*. 12 μm.

4. DISCUSSION

(a) *Morphology of* Amphidinium carterae *cell death*

Chromatin condensation, nuclear disintegration and positive TUNEL labelling precede lysis in *D. tertiolecta* (Segovia *et al.* 2003). By contrast, *A. carterae* undergoes non-specific organellar dissolution and, despite numerous trials, TUNEL testing remained inconclusive or negative. The unusual organization of the dinoflagellate nucleus (e.g. Raikov 1995) may have contributed to the lack of labelling, but this did not prevent labelling in other studies of dinoflagellate cell death (Vardi *et al.* 1999; Dunn *et al.* 2002). However, DNA fragmentation is not definitively diagnostic in the assessment of cell death, not even in metazoan cells; the specificity of DNA fragmentation to apoptosis and necrosis is uncertain (Graslkraupp *et al.* 1995) and probably results from our common inability to confidently distinguish between pre- and post-mortem changes (Jones 2001; Kanduc *et al.* 2002) as well as the high possibility of experimental artefacts (Labat-Moleur *et al.* 1998; Jerome *et al.* 2000). Apoptosis and necrosis morphotypes may well represent a continuum from pre- to post-death rather than a dichotamous path splitting before the moment of death (Kanduc *et al.* 2002). Necrotic cell death in metazoan models has been characterized by a loss of plasma membrane integrity (Willingham 1999), and the mortal stain Sytox-green works by detecting failures in plasma membrane integrity. In metazoan cells, necrosis involves cell swelling, whereas in our study *A. carterae* cells shrank during cell death. Dinoflagellates possess cellulose plates overlying the plasmalemma (Van den Hoek *et al.* 1995) (an obvious difference with typically naked metazoan cells) and the presence of thecal vesicles may account for the lack of cell expansion as cells died. This fundamental difference between a unicellular eukaryotic cell and metazoan cell structure underlines the need for caution in attempting to transfer cell death paradigms from metazoan

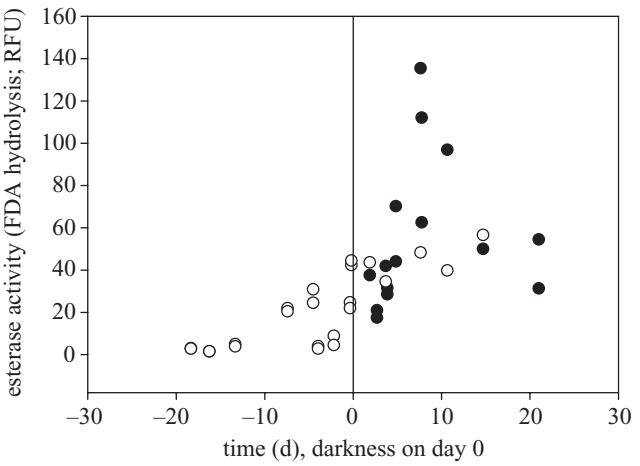

Figure 5. Esterase activity in *Amphidinium carterae* cells transferred to darkness on day 0. Open circles indicate esterase activity in cultures kept in the light, whereas filled circles show esterase activity in cultures transferred to darkness on day 0. Esterase activity was measured as FDA hydrolysis and is presented in relative fluorescence units (RFU). One culture remained in the light (see open circles) after the transfer to darkness. Data are drawn from three independent cultures.

to unicellular eukaryotes. Paraptosis is a PCD-induced morphotype characterized by extensive vacuolization without DNA fragmentation (Sperandio *et al.* 2000). Paraptosis is therefore similar to the process of cell death in *A. carterae*. The rapid vacuolization and loss of internal structure was one of the most striking features of *A. carterae* cell death and is similar to the morphotype of cell death found in the amoeba *Dictylostelium*; when killed through starvation (as *A. carterae* was in the present study through energy limitation), *Dictylostelium* undergoes massive vacuolization without DNA fragmentation (Olie *et al.* 1998). The morphological data presented in this study support the involvement of a similar process in *A. carterae*. Interestingly, cell death in barley aleurone cells, a process that is part of metazoan development, is morphologically similar; loss of plasma membrane integrity, extensive vacuolization and negative DNA fragmentation characterize cell death (Bethke *et al.* 1999). Other potential dinoflagellate life-history pathways for the cell under energy limitation (e.g. cyst formation) are discussed in S1 in electronic Appendix A.

(b) *Causality of* Amphidinium carterae *cell death*

Shrinkage, loss of motility and loss of pigment content (e.g. figure 4) are defining features of algal senescence in 'old' (i.e. nutrient-limited) algal cells in culture (Freudenthal 1962; Pommerville & Kochert 1981; Prezelin 1982; Fogg & Thake 1987; Kirk 1998). Senescence is thought of as an intrinsic process in higher plants; an essential part of multicellular development (Leopold 1961). In algal studies, the term senescence has been more loosely used to describe cell condition during the period of culture decline (e.g. Fogg & Thake 1987) and previous observations of senescent cells probably included observations of dead cells. For example, dead cells in natural populations of phytoplankton (Veldhuis *et al.* 2001) are similar to senescent cultured cells: both show lowered ('degraded') pigment contents. In our study, *A. carterae* senescence, i.e. cell death in stationary phase cultures, and light-deprived cell death, resulted in a similar dead-cell morphology (figure 4). Was an active and/or programmed process involved? The increased esterase activity exhibited when cells were transferred to darkness, along with the increased protease (LAP) activity, suggest greater metabolic activity during the period of mass mortality. Distinguishing between cellular adaptation to unfavourable conditions; which may involve an increase in protease activity and/or catabolic processes (Vierstra 1993), and identifying cellular phenomena that are the result of cell death requires an ability to precisely pinpoint the moment of death (Jones 2001). This remains a significant challenge in understanding the process of unicellular eukaryote cell death. Because the cultures we used were not axenic, the possibility that bacteria contributed to LAP and esterase measurements remains. The manner of our cell collection (relatively low-speed centrifugation), and the high algal to bacteria biomass ratio in the cultures, suggests that the algal signal was probably dominant. Active cell death, in the general sense of metabolic changes preceding lysis, have been noted in other algal species. Increased enzyme activities (phosphatase activity; Hagen & Kochert 1980) and changes in protein expression (Pommerville & Kochert 1981) in senescent *Volvox carteri* lead to autolysis and cell loss (Kirk 1998). We suggest that active cell death in this sense is probably common throughout dinoflagellates; whether this form of cell death has additional similarities with metazoan cells in terms of caspase involvement remains to be seen. An important point is that dinoflagellate senescence, which can also be thought of as 'natural' cell death (i.e. that which results from energy limitation/starvation), is probably always active in the sense that changed enzyme and protein profiles can be measured before the moment of death. Whether this process is harnessed in an adaptive fashion for cell number regulation, perhaps through intercellular signalling, is an emerging and exciting topic (discussed further in S2 of electronic Appendix A).

We have shown that the dinoflagellate *A. carterae* does not display an apoptotic morphology when it dies in darkness and during culture senescence. This contrasts strongly with the chlorophyte *D. tertiolecta*. *Amphidinium carterae* cell death is probably active and shows similarities with a paraptotic cell death morphotype. Cell death triggered by energy limitation is probably a significant process in the structuring of phytoplankton populations.

We thank Dr M. Segovia and G. McCartney for assistance with the TEM work, and B. Stewart for help with the C/N analyses. Thanks to M. Wills and S. Taylor for technical assistance, and to Radem S. L. and Dr H. Mendoza Guzmán for computer support. D.J.F. was supported by a Department of Education and Learning (Northern Ireland Government) scholarship. Some components of the project were supported by a small grant from the Natural Environment Research Council (UK). We thank the two anonymous reviewers for their excellent comments.

REFERENCES

Agusti, S., Satta, M. P., Mura, M. P. & Benavent, E. 1998 Dissolved esterase activity as a tracer of phytoplankton lysis: evidence of high phytoplankton lysis rates in the northwestern Mediterranean. *Limnol. Oceanogr.* **43**, 1836–1849.

Ameisen, J. C. 2002 On the origin, evolution, and nature of programmed cell death: a timeline of four billion years. *Cell Death Diff.* **9**, 367–393.

Berges, J. A. & Falkowski, P. G. 1996 Cell-associated proteolytic enzymes from marine phytoplankton. *J. Phycol.* **32**, 566–574.

Berges, J. A. & Falkowski, P. G. 1998 Physiological stress and cell death in marine phytoplankton: induction of proteases in response to nitrogen or light limitation. *Limnol. Oceanogr.* **43**, 129–135.

Berges, J. A., Franklin, D. J. & Harrison, P. J. 2001 Evolution of an artificial seawater medium: improvements in enriched seawater, artificial seawater over the last two decades. *J. Phycol.* **37**, 1138–1145.

Bethke, P. C., Lonsdale, J. E., Fath, A. & Jones, R. L. 1999 Hormonally regulated programmed cell death in barley aleurone cells. *Pl. Cell* **11**, 1033–1045.

Brussaard, C. P. D., Riegman, R., Noordeloos, A. A. M., Cadee, G. C., Witte, H., Kop, A. J., Nieuwland, G., van Duyl, F. C. & Bak, R. P. M. 1995 Effects of grazing, sedimentation and phytoplankton cell lysis on the structure of a coastal pelagic food web. *Mar. Ecol. Prog. Ser.* **123**, 259–271.

Brussaard, C. P. D., Gast, G. J., Van Duyl, C. & Riegman, R. 1996 Impact of phytoplankton bloom magnitude on a pelagic microbial food web. *Mar. Ecol. Prog. Ser.* **144**, 211–221.

Cohen, G. M. 1997 Caspases: the executioners of apoptosis. *Biochem. J.* **326**, 1–16.

Cullen, J. J. & Renger, E. H. 1979 Continuous measurement of the DCMU-induced fluorescence response of natural phytoplankton populations. *Mar. Biol.* **53**, 13–20.

Dodge, J. D. 1973 *The fine structure of algal cells*. London: Academic.

Dunn, S. R., Bythell, J. C., Le Tissier, M. D. A., Burnett, W. J. & Thomason, J. C. 2002 Programmed cell death and cell necrosis activity during hyperthermic stress-induced bleaching of the sea anemone *Aiptasia* sp. *J. Exp. Mar. Biol. Ecol.* **272**, 29–53.

Fogg, G. E. & Thake, B. 1987 *Algal cultures and phytoplankton ecology*. University of Wisconsin Press.

Freudenthal, H. D. 1962 Symbiodinium gen. nov. and Symbiodinium microadriaticum sp. nov., a Zooxanthella: taxonomy, life cycle, and morphology. *J. Protozool.* **9**, 45–52.

Gavrieli, Y., Sherman, Y. & Ben-Sasson, S. A. 1992 Identification of programmed cell death *in situ* via specific labelling of nuclear DNA fragmentation. *J. Cell Biol.* **119**, 493–501.

Graslkraupp, B., Ruttkaynedecky, B., Koudelka, H., Bukowska, K., Bursch, W. & Schultehermann, R. 1995 *In situ* detection of fragmented DNA (TUNEL assay) fails to discriminate among apoptosis, necrosis, and autolytic cell death: a cautionary note. *Hepatology* **21**, 1465–1468.

Guillard, R. R. L. & Hargraves, P. E. 1993 Stichochrysis immobilis is a diatom, not a chrysophyte. *Phycologia* **32**, 234–236.

Hagen, G. & Kochert, G. 1980 Protein synthesis in a new system for the study of senescence. *Exp. Cell Res.* **127**, 451–457.

Heiskanen, A. S. 1993 Mass encystment and sinking of dinoflagellates during a spring bloom. *Mar. Biol.* **116**, 161–167.

Hulbert, E. M. 1957 The taxonomy of unarmoured dinophyceae of shallow embayments on Cape Cod, Massachusetts. *Biol. Bull.* **112**, 196–219.

Jerome, K. R., Vallan, C. & Jaggi, R. 2000 The TUNEL assay in the diagnosis of graft-versus-host disease: caveats for interpretation. *Pathology* **32**, 186–190.

Jochem, F. J. 1999 Dark survival strategies in marine phytoplankton assessed by cytometric measurement of metabolic activity with fluorescein diacetate. *Mar. Biol.* **135**, 721–728.

Jones, A. M. 2001 Programmed cell death in development and defense. *Pl. Physiol.* **125**, 94–97.

Kanduc, D. (and 14 others) 2002 Cell death: apoptosis versus necrosis (review). *Int. J. Oncol.* **21**, 165–170.

Kerr, J. F. R., Wyllie, A. H. & Currie, A. R. 1972 Apoptosis: a basic biological phenomenon with wide-ranging implications in tissue kinetics. *Br. J. Cancer* **26**, 239–257.

Kirchman, D. L. 1999 Phytoplankton death in the sea. *Nature* **398**, 293–294.

Kirk, D. L. 1998 *Volvox. Molecular-genetic origins of multicellularity and cellular differentiation*. Cambridge University Press.

Labat-Moleur, F., Guillermet, C., Lorimier, P., Robert, C., Lantuejoul, S., Brambilla, E. & Negoescu, A. 1998 TUNEL apoptotic detection in tissue sections: critical evaluation and improvement. *Histochem. Cytochem.* **46**, 327–334.

Leopold, A. C. 1961 Senescence in plant development. *Science* **134**, 1727–1732.

Maxwell, K. & Johnson, G. N. 2000 Chlorophyll fluorescence: a practical guide. *J. Exp. Bot.* **51**, 659–668.

Ning, S. B., Guo, H. L., Wang, L. & Song, Y. C. 2002 Salt stress induces programmed cell death in prokaryotic organism *Anabaena*. *J. Appl. Microbiol.* **93**, 15–28.

Noble, R. T. & Fuhrman, J. A. 1998 Use of SYBR Green I for rapid epifluorescence counts of marine viruses and bacteria. *Aquat. Microb. Ecol.* **14**, 113–118.

Noji, T., Passow, U. & Smetacek, V. 1986 Interaction between pelagial and benthal during autumn in Kiel Bight. I. Development and sedimentation of phytoplankton blooms. *Ophelia* **26**, 333–349.

Olie, R. A., Durrieu, F., Cornillon, S., Loughran, G., Gross, J., Earnshaw, W. C. & Golstein, P. 1998 Apparent caspase independence of programmed cell death in *Dictyostelium*. *Curr. Biol.* **8**, 955–958.

Pollingher, U. 1987 Ecology of dinoflagellates: freshwater ecosystems. In *The biology of dinoflagellates* (ed. F. J. R. Taylor), pp. 611–648. Oxford: Blackwell.

Pommerville, J. C. & Kochert, G. D. 1981 Changes in somatic cell structure during senescence of Volvox carteri. *Eur. J. Cell. Biol.* **24**, 236–243.

Prezelin, B. B. 1982 Effects of light intensity on aging of the dinoflagellate *Gonyaulax polyedra*. *Mar. Biol.* **69**, 129–135.

Raikov, I. B. 1995 The dinoflagellate nucleus and chromosomes: mesokaryote concept reconsidered. *Acta Protozool.* **34**, 239–247.

Samuelsson, G. & Oquist, G. 1977 A method for studying photosynthetic capacities of unicellular algae based on *in vivo* chlorophyll fluorescence. *Physiol. Pl.* **40**, 315–319.

Segovia, M., Haramaty, L., Berges, J. A. & Falkowski, P. G. 2003 Cell death in the unicellular chlorophyte *Dunaliella tertiolecta*. A hypothesis on the evolution of apoptosis in higher plants and metazoans. *Pl. Physiol.* **132**, 1–7.

Sheldrake, R. 1974 The ageing, growth and death of cells. *Nature* **250**, 381–385.

Smith, P. K., Krohn, R. I., Hermanson, G. T., Mallia, A. K., Gartner, F. H., Provenzando, M. D., Fujimoto, E. K., Goeke, N. M., Olson, B. J. & Klenk, D. C. 1985 Measurement of protein using bicinchoninic acid. *Anal. Biochem.* **150**, 76–85.

Sperandio, S., De Belle, I. & Bredesen, D. E. 2000 An alternative, nonapoptotic form of programmed cell death. *Proc. Natl Acad. Sci. USA* **97**, 14 376–14 381.

Suttle, C. A., Chan, A. M. & Cottrell, M. T. 1990 Infection of phytoplankton by viruses and reduction of primary productivity. *Nature* **347**, 467–469.

Van Boeckel, W. H. M., Hansen, F. C., Riegman, R. & Bak, R. P. M. 1992 Lysis-induced decline of a *Phaeocystis* spring bloom and coupling with the microbial food web. *Mar. Ecol. Prog. Ser.* **81**, 269–276.

Van den Hoek, C., Mann, D. G. & Jahns, H. M. 1995 *Algae: an introduction to Phycology*. Cambridge University Press.

Vardi, A., Berman-Frank, I., Rozenberg, T., Hadas, O., Kaplan, A. & Levine, A. 1999 Programmed cell death of the dinoflagellate *Peridinium gatunense* is mediated by CO_2 limitation and oxidative stress. *Curr. Biol.* **9**, 1061–1064.

Vaux, D. L. & Korsmeyer, S. J. 1999 Cell death in development. *Cell* **96**, 245–254.

Veldhuis, M. J. W., Cucci, T. L. & Sieracki, M. E. 1997 Cellular DNA content of marine phytoplankton using two new fluorochromes: taxonomic and ecological implications. *J. Phycol.* **33**, 527–541.

Veldhuis, M. J. W., Kraay, G. W. & Timmermans, K. R. 2001 Cell death in marine phytoplankton: correlation between changes in membrane permeability, photosynthetic activity, pigmentation and growth. *Eur. J. Phycol.* **36**, 167–177.

Vierstra, R. D. 1993 Protein degradation in plants. *Ann. Rev. Pl. Physiol. Pl. Mol. Biol.* **44**, 385–410.

Walsh, J. J. 1983 Death in the sea: enigmatic phytoplankton losses. *Prog. Oceanogr.* **12**, 1–86.

Willingham, M. C. 1999 Cytochemical methods for the detection of apoptosis. *Histochem. Cytochem.* **47**, 1101–1109.

Wyllie, A. H., Kerr, J. F. R. & Currie, A. R. 1980 Cell death: the significance of apoptosis. *Int. Rev. Cytol.* **68**, 251–303.

As this paper exceeds the maximum length normally permitted, the authors have agreed to contribute to production costs.

Visit www.journals.royalsoc.ac.uk and navigate through to this article in *Proceedings*: Biological Sciences to see the accompanying electronic appendices.